Electronic Supplementary Material (ESI) for New Journal of Chemistry.

SUPPORTING INFORMATION

Fabrication of a solid sensor based on phenazine derivative film for enhancing sensing properties of biogenic amine and applying for monitoring shrimp freshness

Xiao-Ni Qi, You-Ming Zhang, Hong Yao, Qi Lin and Tai-Bao Wei*

Contribution from:

Key Laboratory of Eco-functional Polymer Materials of the Ministry of Education, Key Laboratory of Eco-environmental Polymer Materials of Gansu Province, College of Chemistry 1and Chemical Engineering, Northwest Normal University, Lanzhou, Gansu, PR China

*Corresponding author
Tel: +086 9317973191; E-mail address: weitaibao@126.com.

TABLE OF CONTENTS

Fig. S11 The linear fitting equation and the limitation of PD-6 to various amines, including triethylamine(a), ammonium hydroxide(b), trimethylamine(c), butylamine(d), cholamine (e) and p-aminophenol(f).

Fig. S12 Fluorescence spectrum of PD-6 (2.0×10^{-5} M) in system DMSO/H_2O (2:8, v/v) solution) upon addition 20 kinds amino acid(AA), 10 kinds alcohol and 8 kinds esters in pH =12.

Fig. S13 The SEM images of **PD-6**(A)，**PD-6**+TEA(B) and **PD-6**+TEA +acid(C).

Fig. S14 The HOMO-LUMO of the frontier orbitals for PD-6 and PD-6+various amine including ammonium, TEA, TMA, Butylamine, Cholamine, p-aminophenol.(C: grey, O: red. N: blue). (DFT/B3LYP/6-311G method).

Fig. S15 The MSD curve of **PD-6** film with increasing temperature from 25 ℃ to 85 ℃.

Fig. S16 Water vapor permeability at different time interal from 0 h to 8 h.

Fig. S17 Fluorescence photographs of **PD-6** composites films without the shrimp sample standing for 7 days in the room temperature(~21℃) and Refrigerator(4℃), respectively(RH: ~30%)**.**

Fig. S18 The antibacterial activity of PD-6 film (T=21℃, RH: ~30%).

Fig. S19 The stability in the real application of PD-6 film (T=21℃, RH=~30%).

1. Synthesis of TD, PD-B and PD-6

Potassium iodide (0.83g, 5mmol) and 1, 4-dibromobutane (5.32 g, 25 mmol) were mixed in acetone (250 mL) and intensively stirred for 2 h in the room temperature, then the potassium carbonate (6.9g, 50 mmol) was added in the above solution and continuously stirred 30 min. The *p*-hydroxy benzaldehyde (2.44 g, 20 mmol) was sequentially added in the above solution and stirred for 72 hours in the 60℃ under continuous refluxing. And then cooling to room temperature, the yellow green solution was obtained via vacuum filtration and purified by the column chromatography (silica gel; petroleum: ether = 40:1) to get reddish brown liquid product **TD.**

2,3-diamino phenazine was synthesized according to previous reported method (Wei et al., 2019; Zhang et al., 2019). 2,3-diamino-phenazine (0.42 g, 2 mmol) and acetic acid (1-2 mL) as catalyst were mixed in DMF (20 mL), **TD** (0.64g, 2.5 mmol) was dropwise added in the above solution. The solution was intensively stirred for 18 hours with continuous refluxing, and then cooling to room temperature, the brown precipitate was obtained via filtrating the mixture. Finally, alternately washed with hot absolute ethanol and acetone for three times and recrystallized with DMF/H_2O to get brown powdery product **PD-B**. The synthesis route was displayed in scheme1.

TD: Yield: 50.1%; m.p.61-63℃; ^{1}H NMR (600 MHz, DMSO-d_6, 293 K) of **TD** δ 9.83 ppm (s 1H, CHO), δ 7.83-7.81 ppm (d 2H ArH), δ 7.08-7.07 ppm (d 2H ArH), δ 4.08 (t 2H), δ 3.56 (t 2H), δ 1.94-1.83 (m 4H). The ^{13}C NMR spectrum of **TD** is shown in Fig. S2. ^{13}C NMR (150 MHz, DMSO-d_6, 293 K) of TD δ(ppm): 161.06, 142.94, 129.79, 125.35, 114.76, 67.11,33.29, 29.23, 27.05. ESI-MS m/z: [M+H$^+$] Calcd for $C_{19}H_{12}N_4O_2$ 257.01772; Found 257.01696 as shown in Fig. S3.

PD-B: Yield: 65.3%; m.p.>300℃; 1H NMR (600 MHz, DMSO-d_6, 293 K) of PD-B δ13.22 ppm (s 1H, NH) δ 8.26 ppm (d 2H ArH), δ 8.22 ppm (d 4H ArH), δ 7.85 ppm (d 2H ArH), δ 7.17 ppm (s 2H ArH), δ 4.16-4.09 (t 4H), δ 1.84-1.75 (m 4H), ESI-MS m/z: [M+H+] Calcd for C23H20N4OBr 447.08205; Found 447.08151 as shown in Fig. S5.

Compound **PD-6** was synthesized and purified according to literature procedures (Wei et al., 2016; Imato et al., 2020). A solution of **PD-B** (1.78 g, 2 mmol) and potassium iodide (0.37 g, 2mmol) as exchange reagent were mixed in anhydrous acetonitrile (25 mL), 4, 4 '- pyridine (0.15g, 1 mmol) was dropwise added in the above solution. at 85 °C. The solution was intensively stirred for 48 hours with continuous refluxing, and then cooling to room temperature, the dark brown precipitate was obtained via filtrating the mixture. The synthesis route was displayed in scheme S1. **PD-6:** Yield: 49.2%; m.p.>300℃; ^{1}H NMR (600 MHz, DMSO-d_6, 293 K) of **PD-6** δ13.27 ppm (s 2H, NH), δ 9.24 ppm (d 2H ArH), δ 8.62 ppm (d 4H ArH), δ 8.29 ppm (d 4H ArH), δ 8.0 (d 2H ArH), δ 7.86 ppm (d 8H ArH), δ 7.18 ppm (d 8H ArH), δ 4.74 ppm (t 4H), δ 4.14 ppm (t 4H), δ 2.15 ppm (m 4H), δ 1.78 ppm (m 4H). ESI-MS m/z: $[M+OH]^-$ Calcd for $C_{56}H_{47}N_2O_3$ 907.38261; Found 907.38259 as shown in Fig. S6.

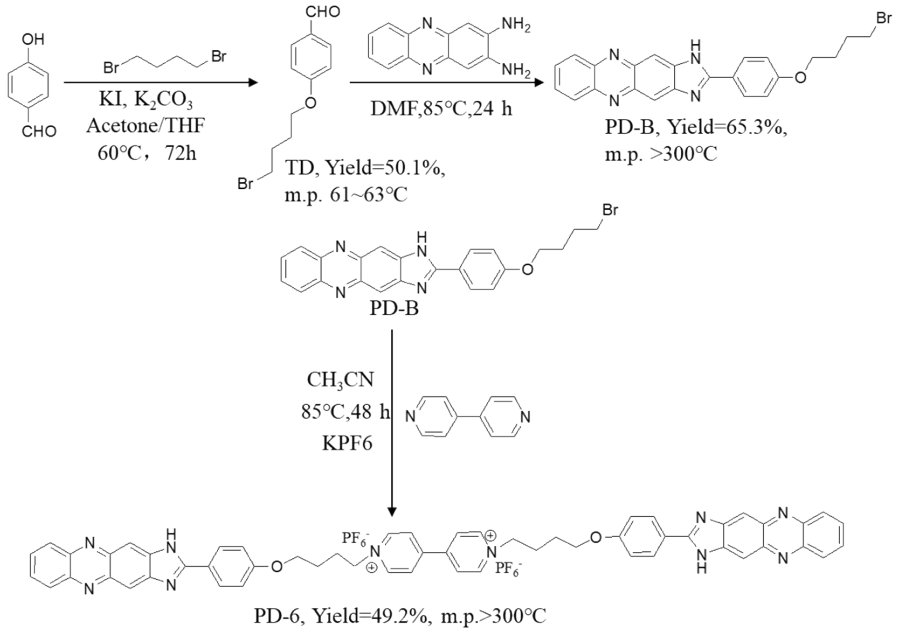

Scheme S1 Synthesis of compound **TD-B, PD-B** and **PD-6**

2. Investigation of optimum emission wavelength and solvent screening

Powdered sample of the **PD-6** (5 mmol) were dispersed respectively in different solvent to obtain suspension (2×10^{-4} M). And then corresponding luminescent measurements were performed immediately. As shown in Fig. S7a-b, the PD-6 could dissolve completely in the DMSO and DMF solvent, but present a strong fluorescence emission (λex=400 nm) with light yellow only in the DMSO solution. According to this observation, the DMSO has been served as the optimal solvent (excitation wavelength λex=400 nm) to investigate the following sensing performance. Meanwhile, the fluorescence stability of **PD-6** in different water fraction were investigated, the corresponding tests were carried out carefully. As shown in Fig. S8, the fluorescence intensity of **PD-6** gradually enhanced after adding the water from 0% to 20%, and then sharply weaken with the water fraction from 20% to 90% accompanied with the color change from the yellow green to dark blue. Therefore, the DMSO/H_2O (2:8 v/v) system was selected as the optimal mixed solvent of the **PD-6** fluorescence sensor and following investigations were performed in above system.

3. Investigation of the mechanical properties of PD-6

The thickness of film samples was determined by using a digital micrometer (Digimatic Micrometer, QuantuMike IP 65, Mitutoyo Corporation, Kanagawa, Japan) with a precision of 1 μm. Five random locations around each film sample were measured and their average value was obtained as the final thickness of **PD-6 film**.

Besides, mechanical properties including the elasticity test, and rheological properties and thermal stability of the **PD-6** film were characterized. Firstly, the elasticity test was performed at room temperature, the original **PD-6** membrane was cut into a cylindrical (2cm×2cm), the reversibility of the elasticity was observed by posing the certain stress. Meanwhile, the control array also has been treated as the similar way. And then, rheological properties were further to illustrated elasticity modulus and thermal stability by using the Rheology instrument (Model 5565, Instron Engineering Corporation, Canton, MA, USA). The film sample was heated to liquid state and was quickly put into the gel

bottle (scale: 5 ml). After cooling to room, those bottles were enclosed in the small tank of rheology instrument and set up the parameters (Temp: from 25-85℃, time: 0-6 h). Afterwards, the resulting elasticity curves were obtained. The G'/G" curves represent the elasticity of the film materials, with the shorter plateaus of the G'/G" curves indicating the higher elasticity of the gels. The elasticity modulus also represents the tolerance of stress, with higher this curve, suggesting the good elasticity index. The mean-squared displacement (MSD) curves represent the elasticity of the gelatin film, with the lower plateaus of the MSD curves indicating the higher elasticity.

4. Water vapor permeability (WVP)

Water vapor permeability (WVP) of the film was determined gravimetrically according to the standard method of ASTM E96-95(Lee et al., 2018). For this, a film sample (5 cm×5 cm) was mounted on the top of the WVP cup (2.5 cm depth and 5 cm diameter) containing 18 mL of distilled water and tightly sealed. The assembled cups were placed in a humidity chamber controlled at 25℃ and 30% RH, and the weight change of the cup was measured at 1 h interval for 8 h period. The WVP (g.m/m^2.Pa.s) of the film was calculated as follows:

$$WVP/\% = (\Delta W \times L)/t \times A \times \Delta p$$

where ΔW was the weight change of the WVP cup (g), L was the mean film thickness (m), t: was the time (s), A was the permeation area of the film (m^2), and Δp was the partial water vapor pressure difference (Pa).

5. Antibacterial activity

The antibacterial activity of the film was examined according to the reports (Roy et al., 2019). Firstly, the PD-6 film solution state or PD-6 film and the control film solution or the control film without adding the PD-6 was casted in the agar plates as shown in Fig S18. And then, cooling to the room temperature, the petri dish was placed in the similar

conditions with process of food freshness detection (Temperature: ~21℃, RH: ~30%). Subsequently, the antibacterial effect was monitored and estimated periodically (0, 3, and 7 d) by counting total viable colony count on the surface of the samples on agar plates.

6. Applied stability tests

In order to verify the stability of **PD-6** film in the process of food freshness detection, the film was made into a roundness with the area of 4 cm^2 and place in the plastic case storing at room temperature (~21 ℃) for 7 days, and the control array was assigned as the with shrimp sample and **PD-6** film. By observing the color change during the 7 days to estimate the stability in the real application as shown in Fig S19.

7. Shrimp freshness trial

Shrimp samples (50 g) were put into plastic case (12.2cm × 4.2 cm) and stored at 21℃ and 4℃ for different time. The indicator films were stuck inside the cap of shrimp sample which had not directly contacted the shrimp. The control group was used without the shrimp samples. There were 10 repeated trays for each sampling day.

8. Calculation of the Limit of Detection (LOD)

The following equations are used to determine the limit of detection (LOD): Equation of linear fitting: y=Ax+B

$$\sigma = \sqrt{\frac{(I_i - \bar{I})^2}{\mathrm{n}-1}} \qquad (i = 1,2 \ldots) \qquad (1)$$

$$S = \frac{I}{Q} \qquad (2)$$

$$LOD = \frac{3\sigma}{S} \qquad (3)$$

9. Computational Methods

Density Functional Theory (DFT) has been used to optimize the ground state geometries. After finishing a configuration optimization and running the harmonic vibrational frequencies, the above results were computed again to acquire the performed

steric configuration. The absence of imaginary frequencies proved that the optimization was successfully completed by chosen appropriate method and basis set. Moreover, the calculation results of the HOMO-LUMO frontier orbitals could offer the ground state optimization configuration. Computation results manifested that the gap energy of **PD-6** was much more than the PD-6+alkalin as shown in Fig. S14, which indicated that the **PD-6** is prone to bind the alkaline compound. All the computations were operated by Gaussian 09 program by using B3LYP method combined with the 6-311G** (d, p) basis set. Visual configuration model of the structures was presented by Gauss View 6.0 program.

10. Statistical analysis

All the experiments were carried out three times at least and the results have been shown in the way of a mean ± standard deviation. the significant difference ANOVA was used to performed according to the Student's t-test at the 90% confidence level applying the statistical analysis program (SPSS Inc., Chicago, IL, USA).

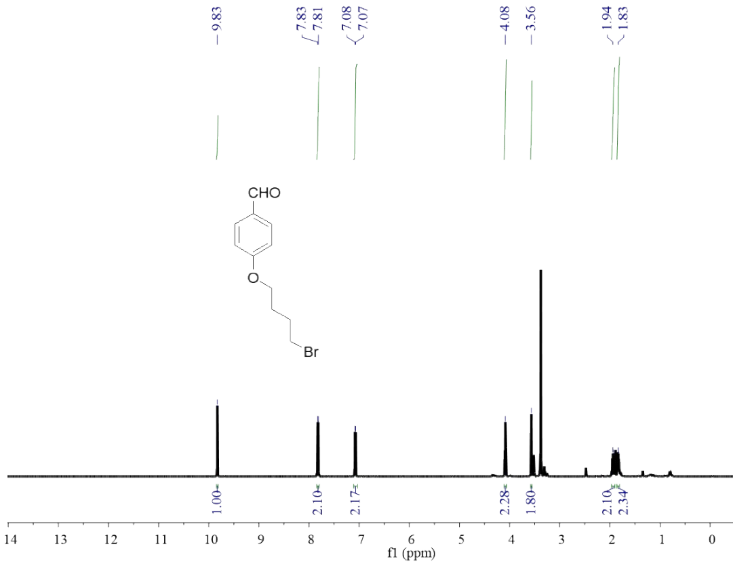

Fig. S1 ^{1}H NMR spectrum (600 MHz, DMSO-d_6, 293 K) of TD

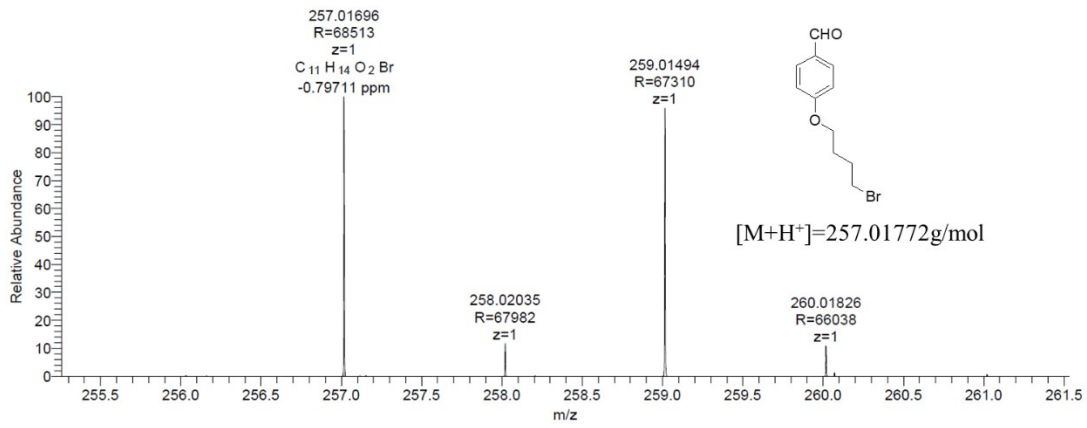

Fig. S2 The ESI-MS of TD: [M+H$^+$] = 257.01772 (ESI-MS m/z: [M+H$^+$] Calcd for $C_{19}H_{12}N_4O_2$ 257.01772; Found 257.01696)

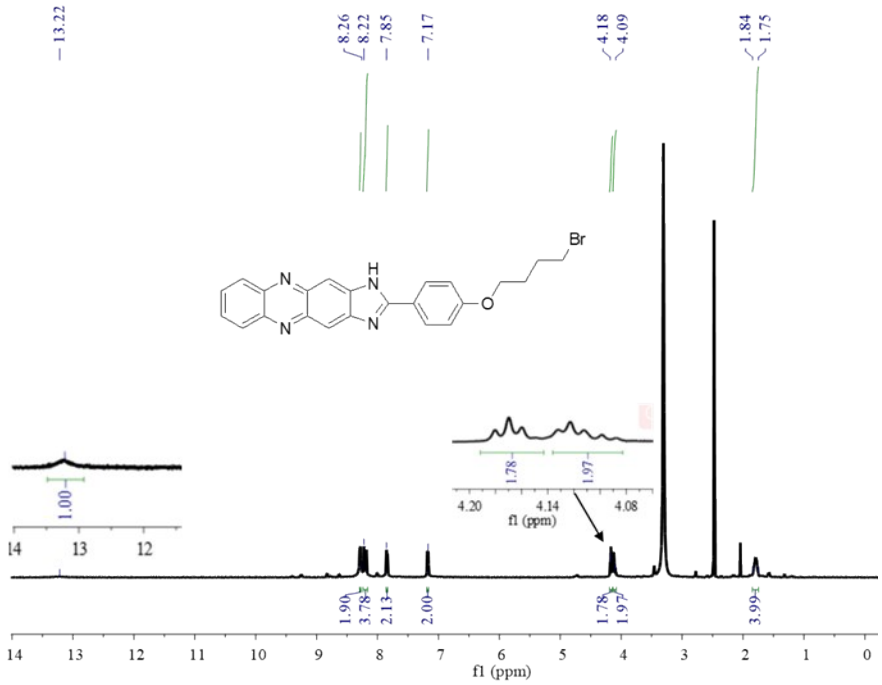

Fig. S3 ^{1}H NMR spectrum (600 MHz, DMSO-d_6, 293 K) of PD-B

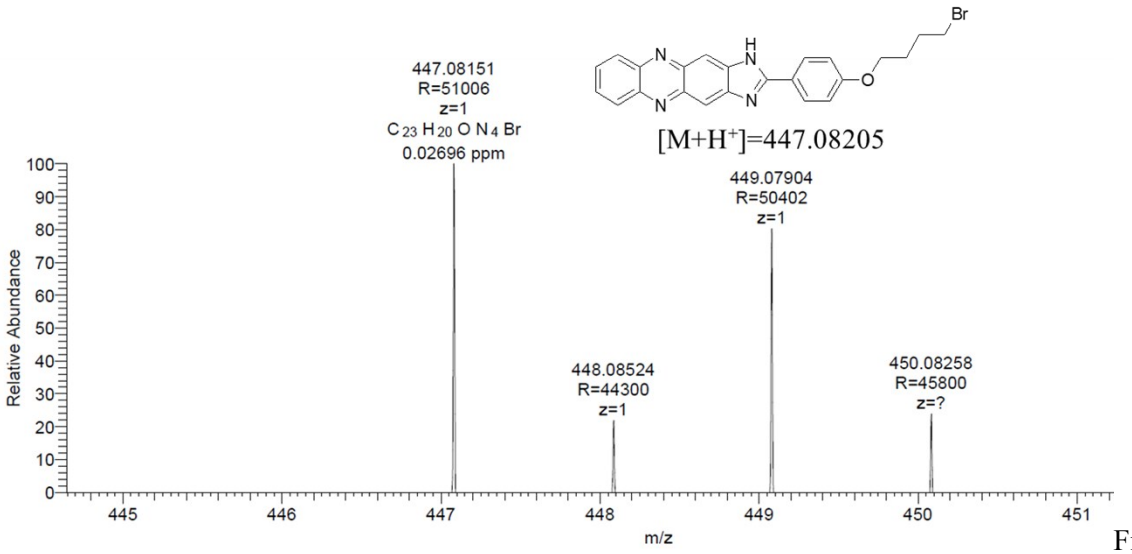

Fig. S4 The ESI-MS of PD-B: [M+H$^+$]=447.08151(ESI-MS m/z: [M+H$^+$] Calcd for $C_{23}H_{20}N_4OBr$ 447.08205; Found 447.08151).

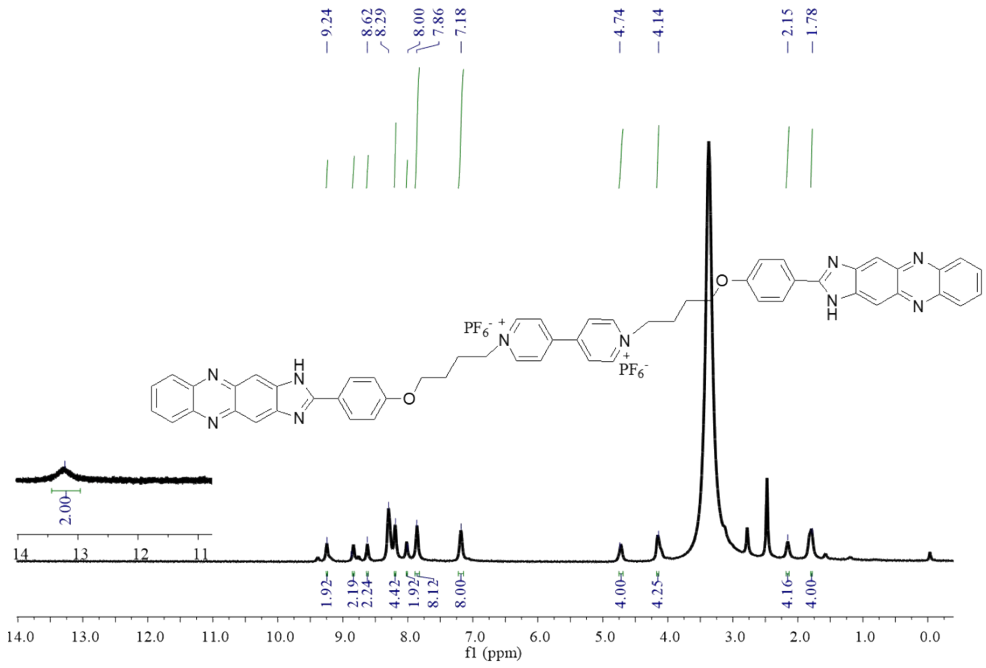

Fig. S5 ^{1}H NMR spectrum (600 MHz, DMSO-d_6, 293 K) of PD-6

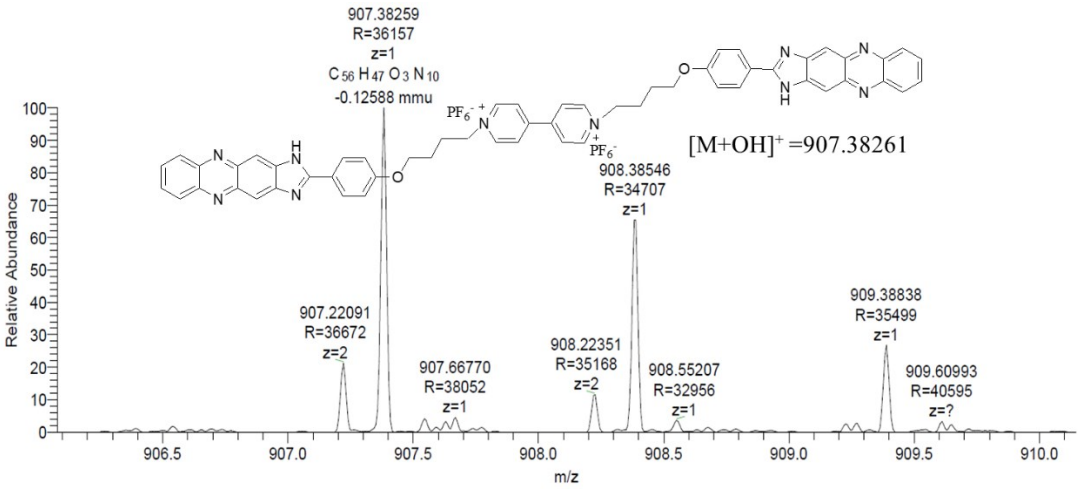

Fig. S6 The ESI-MS of PD-6: $[M+OH]^-$ = 907.38259 (ESI-MS m/z: $[M+OH]^-$ Calcd for $C_{56}H_{47}N_2O_3$ 907.38216; Found 907.38259.

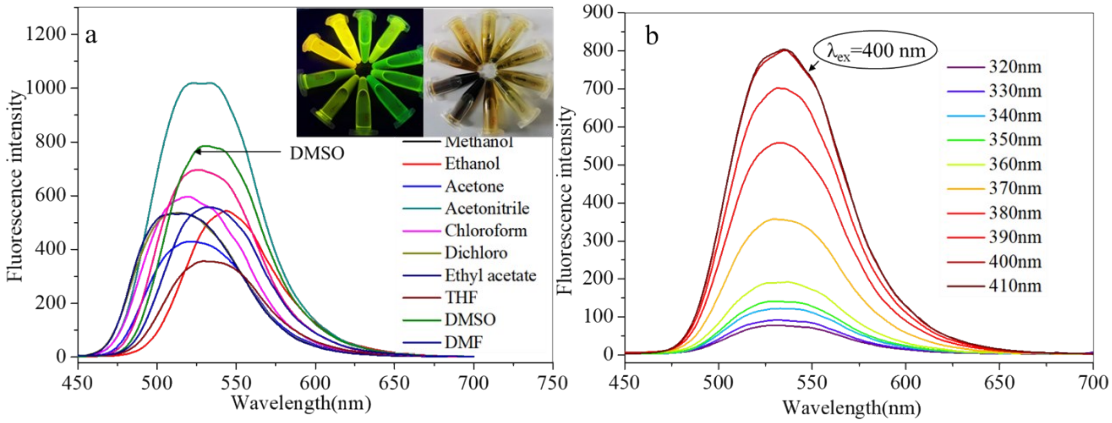

Fig. S7 The fluorescence spectrum and solubility of PD-6 at different sovlents. From 1 to 10: Methanol, Ethanol, Acetone, Acetonitrile, Chloroform, Dichloro, Ethyl acetate, THF, DMSO, DMF; (a) The fluorescence spectrum of PD-6 at different excition wavelength in DMSO solution. From 320 nm to 410 nm(b).

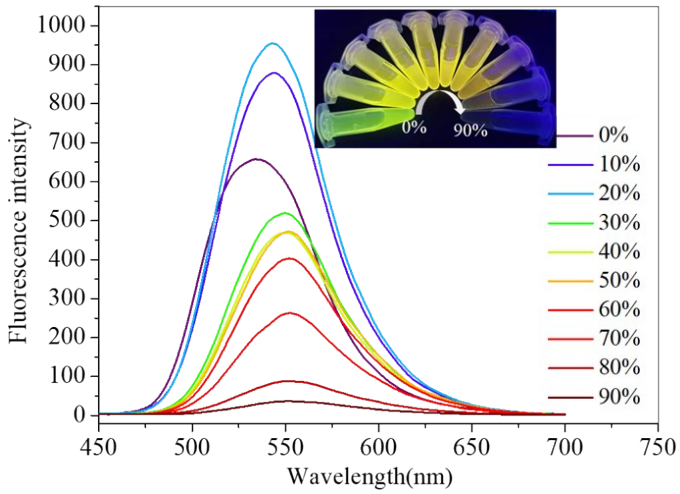

Fig. S8 The fluorescence spectrum of PD-6 at different water volume fractions (Vol%). Insert: the corresponding fluorescence photographs at different water volume fractions from 0% to 90%.

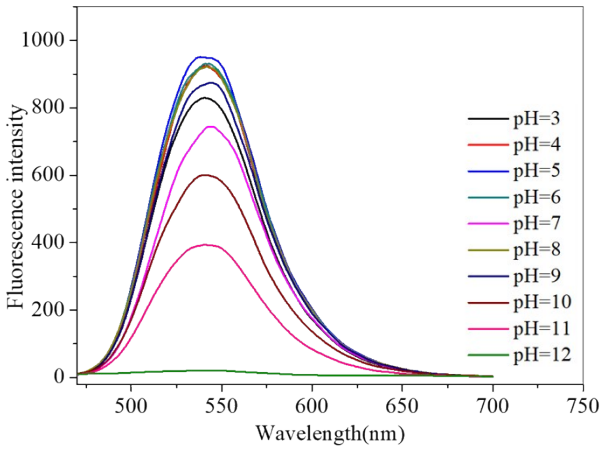

Fig. S9 The response fluorescence spectrum PD-6 (20 μM) at different pH.

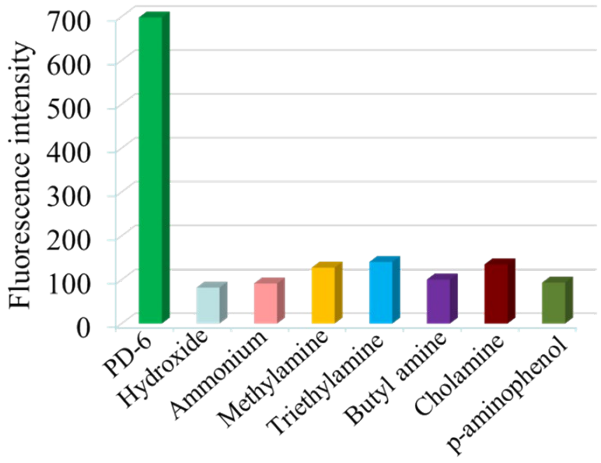

Item	Dissociation constant	pK_b(pOH)
Sodium hydroxide	-	2.0
Ammonium	1.78×10^{-5}	4.78
Methylamine	4.17×10^{-4}	3.38
Triethylamine	6.31×10^{-4}	3.28
Butyl amine	4.37×10^{-4}	3.36
Cholamine	3.16×10^{-5}	4.50
p-aminophenol	2.0×10^{-4}	3.70

Fig. S10 The fluorescence intensity of **PD-6** at different alkaline compound with same equivalent.

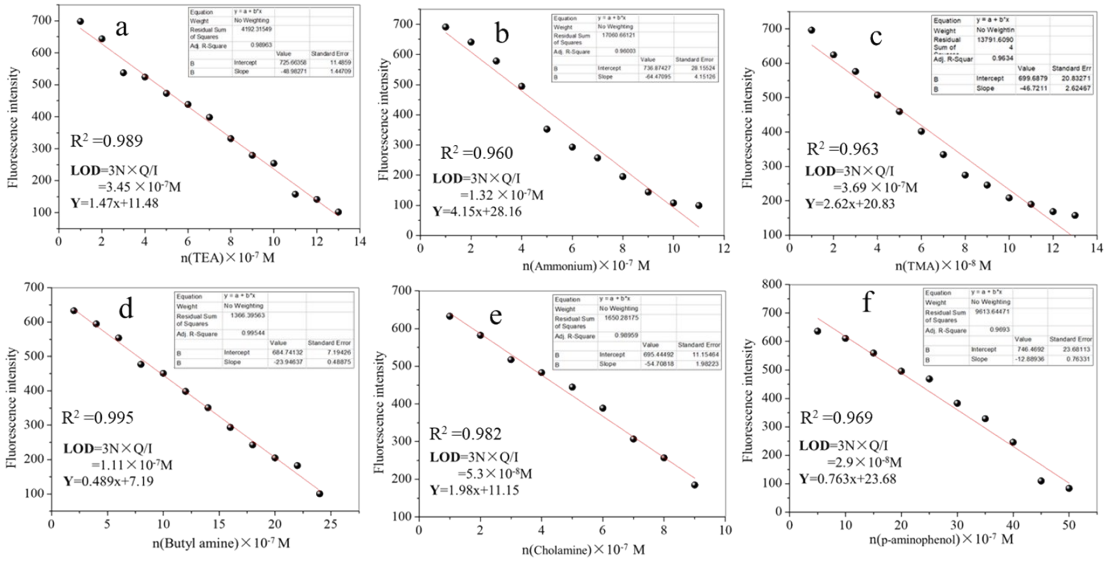

Fig. S11 The linear fitting equation and the limitation of PD-6 to various aminea including the triethylamine(a), ammonium hydroxide(b), trimethylamine(c), butylamine(d), cholamine (e) and p-aminophenol(f).

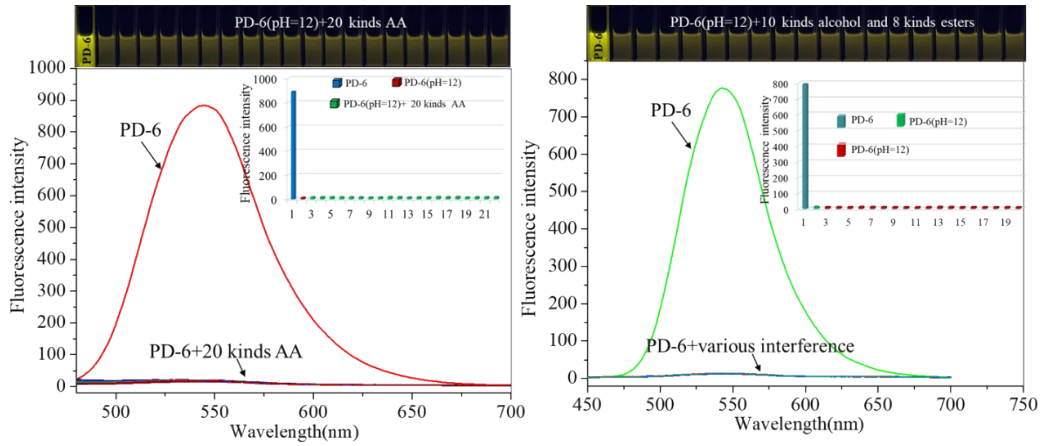

Fig. S12 Fluorescence spectrum of **PD-6** (2.0×10^{-5} M) in system DMSO/H_2O (2:8, v/v) solution upon addition 20 kinds amino acid(AA), 10 kinds alcohol and 8 kinds esters in pH =12.

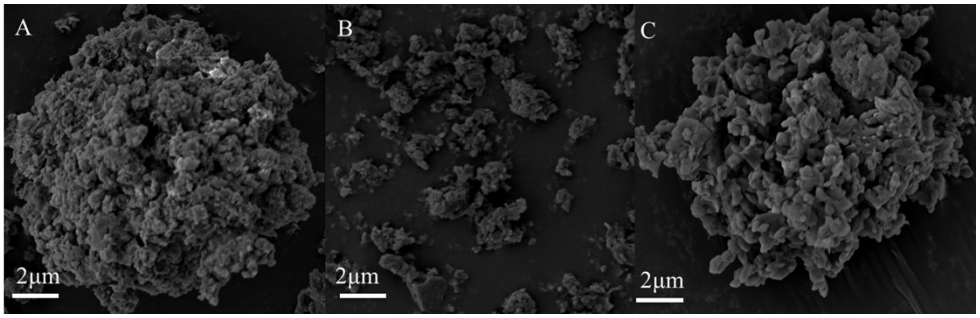

Fig. S13 The SEM images of **PD-6**(A)，**PD-6**+TEA(B) and **PD-6**+TEA +acid(C).

a 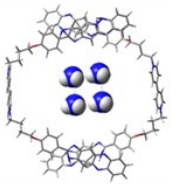	b 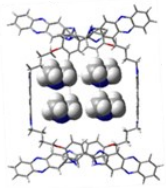	c 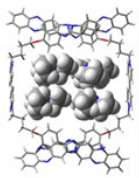
ΔE= 0.18919 eV	ΔE= 0.19060 eV	ΔE= 0.19559 eV
d 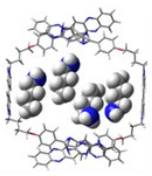	e 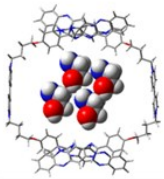	f 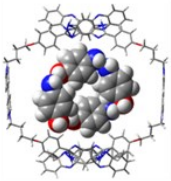
ΔE= 0.19007 eV	ΔE= 0.18115 eV	ΔE= 0.19191eV

Fig. S14 The computational-mimicking binding energy of PD-6 interacted with various amines (a: Ammonium; b: TEA; c: TMA; d: Butylamine; e: Chloramine; f: p-aminophenol) (C: grey, O: red.

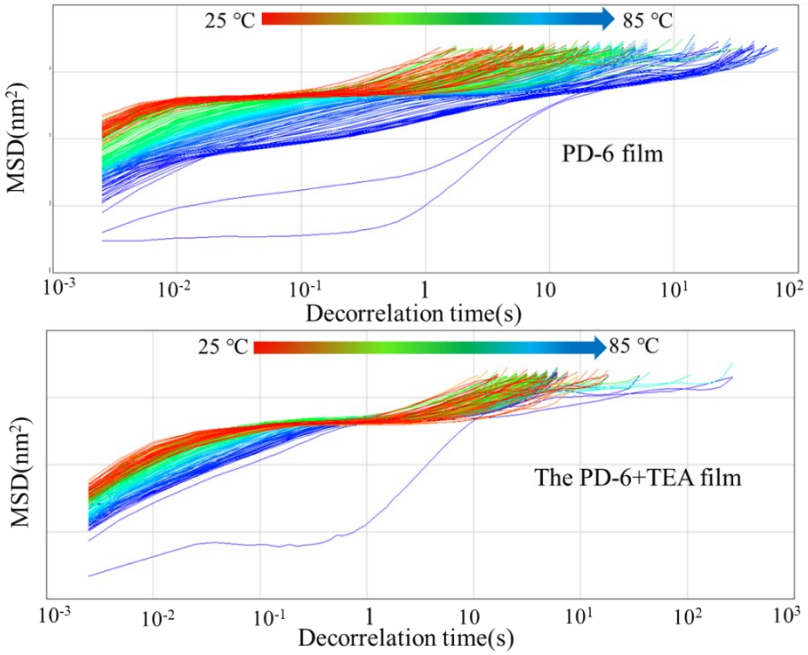

Fig. S15 The MSD curve of PD-6 film with increasing temperature from 25 ℃ to 85 ℃.

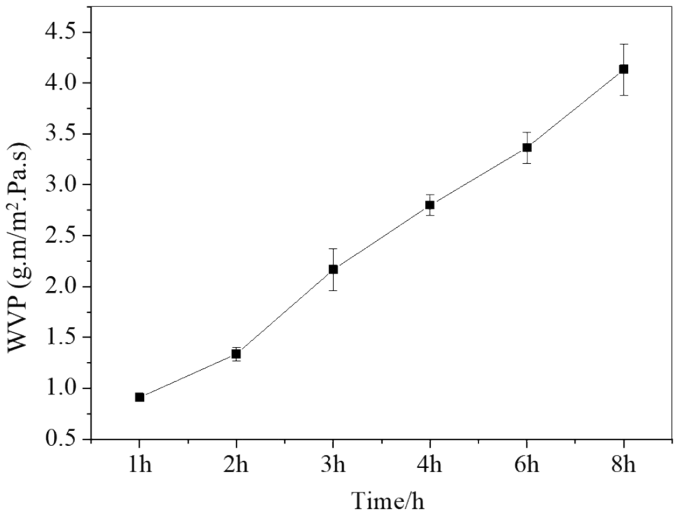

Fig. S16 Water vapor permeability at different time interal from 0 h to 8 h.

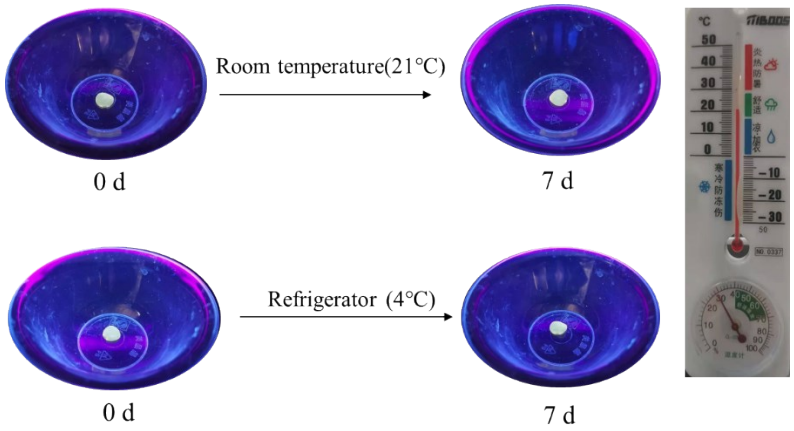

Fig. S17 Fluorescence photographs of **PD-6** composites films without the shrimp sample standing for 7 days in the room temperature(21℃) and refrigerator(4℃), respectively(RH :30%).

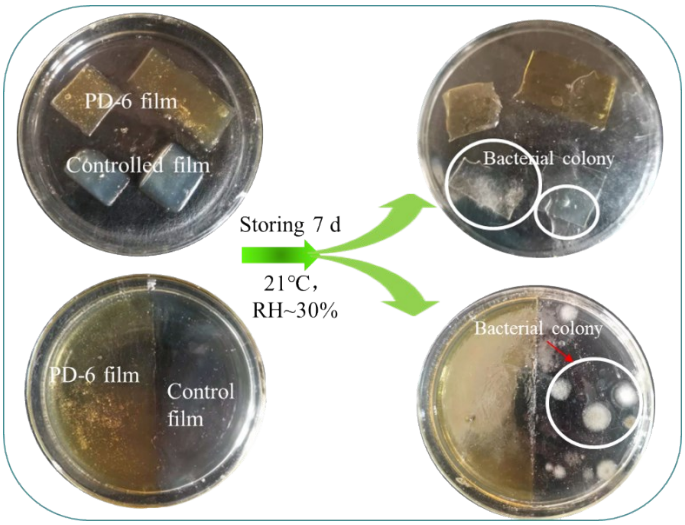

Fig. S18 The antibacterial activity of PD-6 film (T=21℃, RH~30%).

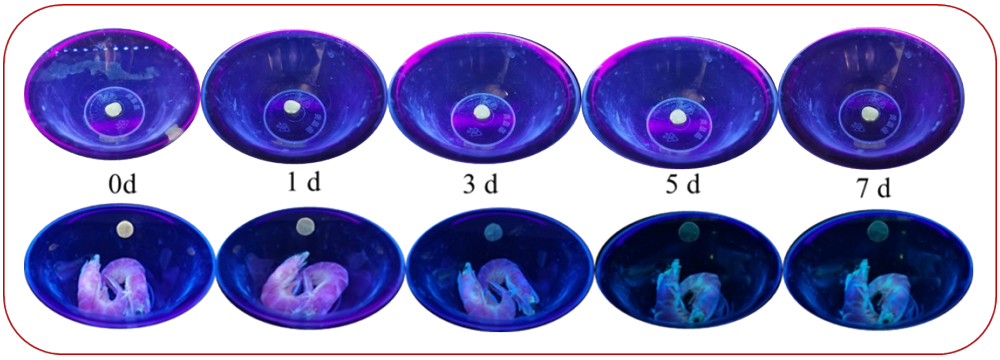

Fig. S19 The stability in the real application of PD-6 film (Temp: ~21℃, RH: ~30%).

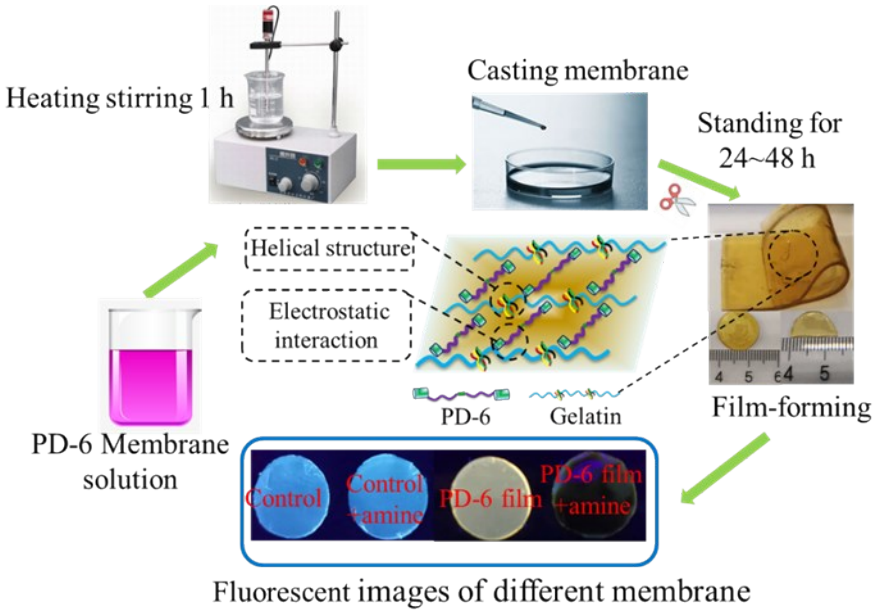

Scheme S2. The diagram of preparation membrane materials

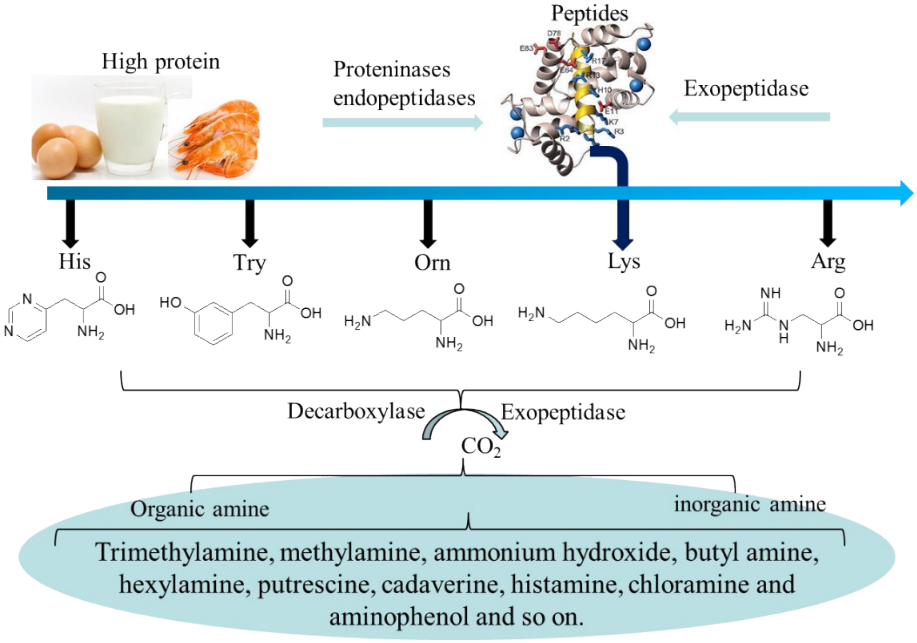

Scheme S3 The decomposition diagram of BAs

Reference:

Imato, K., Yamanaka, R., Nakajima, H. & Takeda, N. (2020). Fluorescent supramolecular mechanophores based on charge transfer interaction. *Chem. Commun, 56,* 7937-7940.

Lee, M. H., Kim, S. Y., & Park, H. J. (2018). Effect of halloysite nanoclay on the physical, mechanical, and antioxidant properties of chitosan films incorporated with clove essential oil. *Food Hydrocolloids, 84,* 58–67.

Wei, T. B., Yong, B. R., Dang, L. R., Zhang, Y. M., Yao, H., & Lin, Q. (2019). A simple water-soluble phenazine dye for colorimetric/fluorogenic dual-mode detection and removal of Cu^{2+} in natural water and plant samples. *Dyes Pigments, 171,*107707.

Wei, T. B., Zhang, H. L., Li, W. T., Qu, W. J., Su, J.X., Lin, Q., Zhang, Y. M., & Yao, H. (2016). A turn-on fluorescent chemosensor selectively detects cyanide in pure water and food sample. *Tetra. Lett, 57,* 2767–2771.

Roy, S., Shankar, S., & Rhim, J.-W. (2019). Melanin-mediated synthesis of silvernanoparticle and its use for the preparation of carrageenan-based antibacterial films. *Food Hydrocolloids, 88,* 237–246.

Zhang, Y. M., Fang, H., Zhu, W., He, J. X., Yao, H., Lin, Q., & Wei, T. B. (2019). Ratiometric fluorescent sensor based oxazolo-phenazine derivatives for detect hypochlorite via oxidation reaction and its application in environmental samples. *Dyes Pigments.172,*107765.